PHOTONICS PUBLIC PRIVATE PARTNERSHIP

INNODERM

687866 —H2020-ICT-2015

D3.2: Report on First Single Element Transducer Implementation

Deliverable nature:	*Other*
Contractual delivery date:	08.2018
Actual delivery date:	06.2019
Version:	2.0

Dissemination level (select one)		
PU	Public	x
PP	Restricted to other programme participants (including the Commission Services)	
RE	Restricted to a group specified by the consortium (including the Commission Services)	
CO	Confidential, only for members of the consortium (including the Commission Services)	

Lead beneficiary: **TUM**

Author(s): **Juan Aguirre.**

Organisation: Technical University of Munich (TUM)
E-mail: juanaguir@gmail.com
Phone: +49 (0) 89 4140 9156

Table of Content

1) Purpose of this document

This document reports on the implementation of the first single element transducer for the scanner that is based on single element transducer technology. Two systems were initially built. System 1 is a lab system, i.e. a system meant to be used by specialized users in a laboratory environment or in a clinic. This lab system was built by TUM and is used in TUMs clinic. In parallel, a second system, System 2, was built by iThera. This system was developed to be used by non-specialized users after being trained on it.

2) System 1: Lab system

To study the abilities of raster-scan optoacoustic mesoscopy (UWSB RSOM) in the visible near infrared range, we built an in-house system. The main components of the system are shown in Figure 1. Optoacoustic signal generation is achieved using a flash-lamp pumped Nd:YAG optical parametric oscillator (SpitLight OPO, InnoLas Laser GmbH, Krailling, Germany). The OPO can be tuned per wavelength from 420 nm to 690 nm in the main operating range, and from 730 nm to 2000 nm range using idler operating range. The emitted light pulse width is 6 ns at a repetition rate of 100 Hz. The system also incorporates two fast single-wavelength lasers. One laser emits pulses at 532 nm wavelength (Wedge HB.532, Bright Solutions, Pavia, Italy), has 0.9 ns pulse width and tunable repetition rate up to 10 kHz. Another fast single-wavelength laser (Flare NX 515 0.6 2, Coherent, Germany) operates at 515 nm wavelength with 1.2 ns pulse width and tunable repetition rate up to 2 kHz. The fast single-wavelength lasers were coupled into one of the inputs of a custom-made fiber bundle (CeramOptec, Riga, Latvia), while the OPO laser was coupled into another input of the fiber bundle. Maximum output energy delivered to the surface of the skin via the fiber bundle were within safety limitations. To detect broadband optoacoustic signals, different focused piezoelectric transducers by Sonaxis can be used and interchanged in a matter of minutes.

The detected optoacoustic signal is amplified using a low-noise amplifier (63 dB; AU-1291, MITEQ, Hauppauge, New York, USA). Analog signals are digitized by a high-speed digitizer (EON-121-G20; Gage Applied Technologies, Montreal, Canada) with a sampling rate of 1 GS/s. The optoacoustic signals are acquired by raster-scanning a detector attached to the precise piezoelectric stages (Physik Instrumente, Auburn, USA).

The fiber bundle outputs, transducer, and moving stages are enclosed in a compact 3D-printed scanning head made of polylactic acid material. A small compartment in the interface unit is filled with a coupling medium and is located at the bottom of the scanning head. The interface unit can be affixed to a desired imaging area in a user friendly manner. The ease of use of the interface unit and the fast acquisition time (~1min) makes the system compatible with clinical research use.

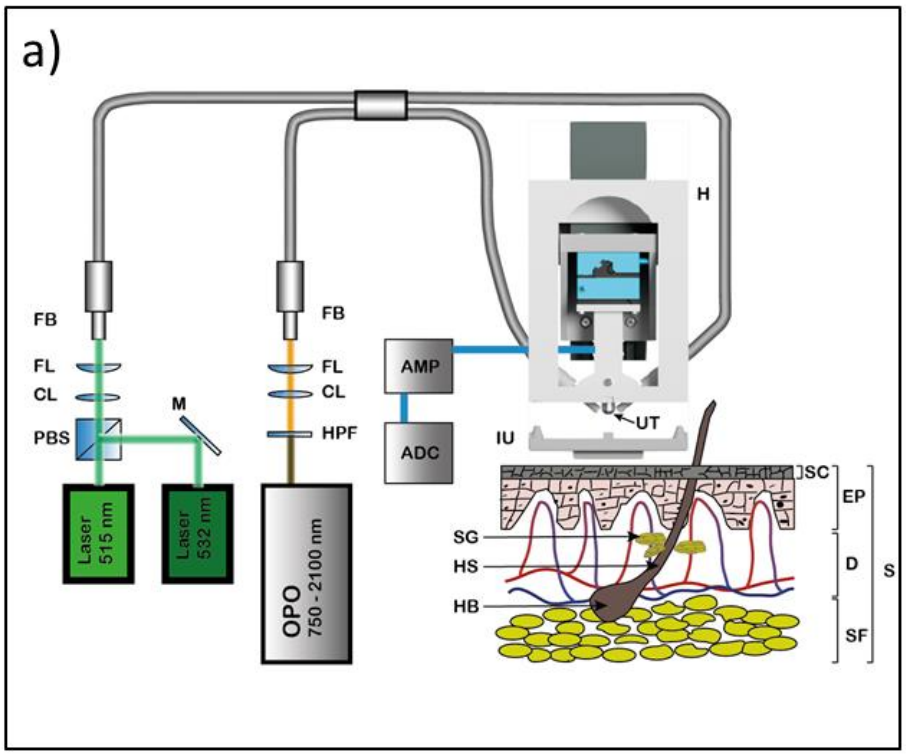

Figure 1: a. Schematics of UWSB RSOM and experimental design. FB – fiber bundle, FL – focusing lens, CL – collimating lens, PBS – polarizing beam splitter, M – mirror, HPF – high pass filter; ADC – analog – to – digital converter, AMP – 60 dBm amplifier, IU – detachable interface unit, UT – ultrasound transducer, H – RSOM holder; S – schematic of human skin, EP – epidermis, D – dermis, SF – subcutaneous fat, SG – sebaceous glands, HS – hair shaft, HB – hair bulb.

3) System 2: System by iThera Medical

The system built by iThera Medical which is intended to be disseminated to different laboratories around the world is called RSOM Explorer C50. It consists of a clinical cart with galvanic transformer, a workstation, wireless keyboard and mouse, LED monitor, a laser box, and a positioning arm with scan head (Figure 2). According to IEC 60825-1, the system is a class 4 laser product.

The system cart contains platforms for the main components of the RSOM Explorer. The clinical cart is equipped with a power supply including a galvanic transformer to provide galvanic isolation and to limit leakage currents. The system is meant to be operated in standing position. Therefore, a place for mouse and keyboard is embedded at a suitable height. The power supply provides 110-230VAC, 50/60 Hz, 1600VA maximum to the RSOM workstation, laser box, and monitor. The main ON-OFF switch is placed at the right side of the cart. System manoeuvrability is provided by four swivel wheels. Pedal locks on the wheels prevent the cart from moving during operation.

The workstation provides image acquisition and reconstruction, data storage, besides configuration and communication among all modules of the RSOM system. The flat-panel monitor at the top of the cart is a 24-inch colour display with a resolution of 1920 x 1200 pixel. The monitor mount allows for tilt and swivel to adjust the display position. Wireless keyboard and mouse are used as the main user interface to the RSOM system.

The data acquisition card (DAQ) is placed inside the RSOM workstation. It converts analog voltages from the acoustic transducer into digital data to be recorded by the viewRSOM software. Only one of the two channels of the DAQ is used by the system. Data acquisition is triggered by a photodetector.

The laser box contains the laser cavity, the power supply distribution, the laser safety features, and the triggering photodetector. The laser control box is attached on top of the laser box. It communicates with the laser box, stage controller and RSOM workstation.

To perform precise raster-scanning and trigger laser pulse emission, the system has implemented automatically controlled scan stages. The stage controller is also attached on top of the laser box.

To position the scan head precisely on the region of interest, it is mounted on a spring-loaded microscope arm. The microscope arm enables horizontal, vertical, rotation, and tilting movements. The horizontal movement joints are friction joints. To prevent motion of the scan head during imaging, all other joints should be locked.

The main imaging part of the RSOM is the scan head. It contains fast piezo micro positioning stages and a single element ultrasound transducer that is mounted at the tip of the scan head. It detects ultrasound waves and converts them into the electrical signals. Those electrical signals are transmitted to an amplifier and further to the DAQ card.

Following the IEC standard for medical devices, several safety features are implemented in the scanner, including LEDs indicating power on, laser ready, and laser emission, a key switch and a safety emergency switch, an external interlock connector (can for example be used for a door interlock), a foot pedal interlock, as well as an external laser warning light connector (can be connected to external laser warning lights).

The ease of use of the scan head position system, plus the fast acquisition times (~1min) makes the system compatible with clinical research use.

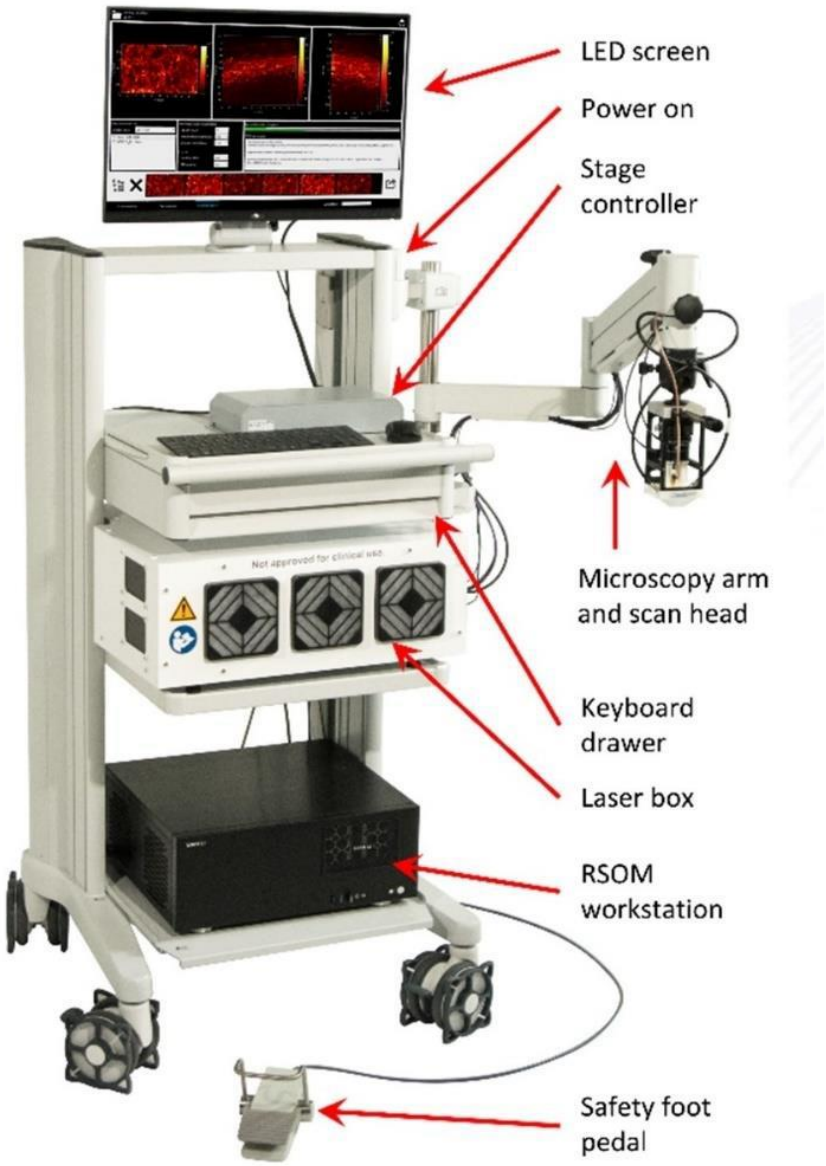

Figure 2. RSOM Explorer C50 by iThera Medical

4) In vivo imaging

This section presents some in vivo images taken with the lab system (System 1) from different skin lesions and pathologies.

We demonstrate the appearance of eczema, which is associated with a strong inflammatory process. The cross sections corresponding to skin areas affected by eczema of two different patients (Figure 3a and b) exhibit different degrees of acanthosis and elongated capillary loops. Differences in the vascular structures in the dermis can be clearly observed. In Fig.3c-g we show the quantification of different vascular and epidermal properties corresponding to three eczema patients. The features resolved included the total blood volume, epidermis thickness, fractal number, density of capillaries and capillaries diameter. Such features can be used as precision biomarkers for disease severity evaluation and can be particularly useful for allergy testing which is commonly driven by subjective visual observations.

Figure 3h shows a cross section of healthy skin in which a hair shaft can be observed together with its surrounding vessels. The length of the hair inside the skin is ~2mm. The ability to image hair follicles and their vascular environment may be useful in the examination on alopecia and acne. The ability to image nevi and its underlying vascular structure is showcased in Fig. 3i. The nevi can be clearly observed in the epidermis. Eventual changes in the shape and size of the nevi, or in the surrounding vessel structure, can be a sign of malignant transformation. Finally, the RSOM cross section of a skin area affected by vasculitis is shown in Fig. 3j. The vessel structure appears completely distorted and corresponds to the clinical phenotype of the condition.

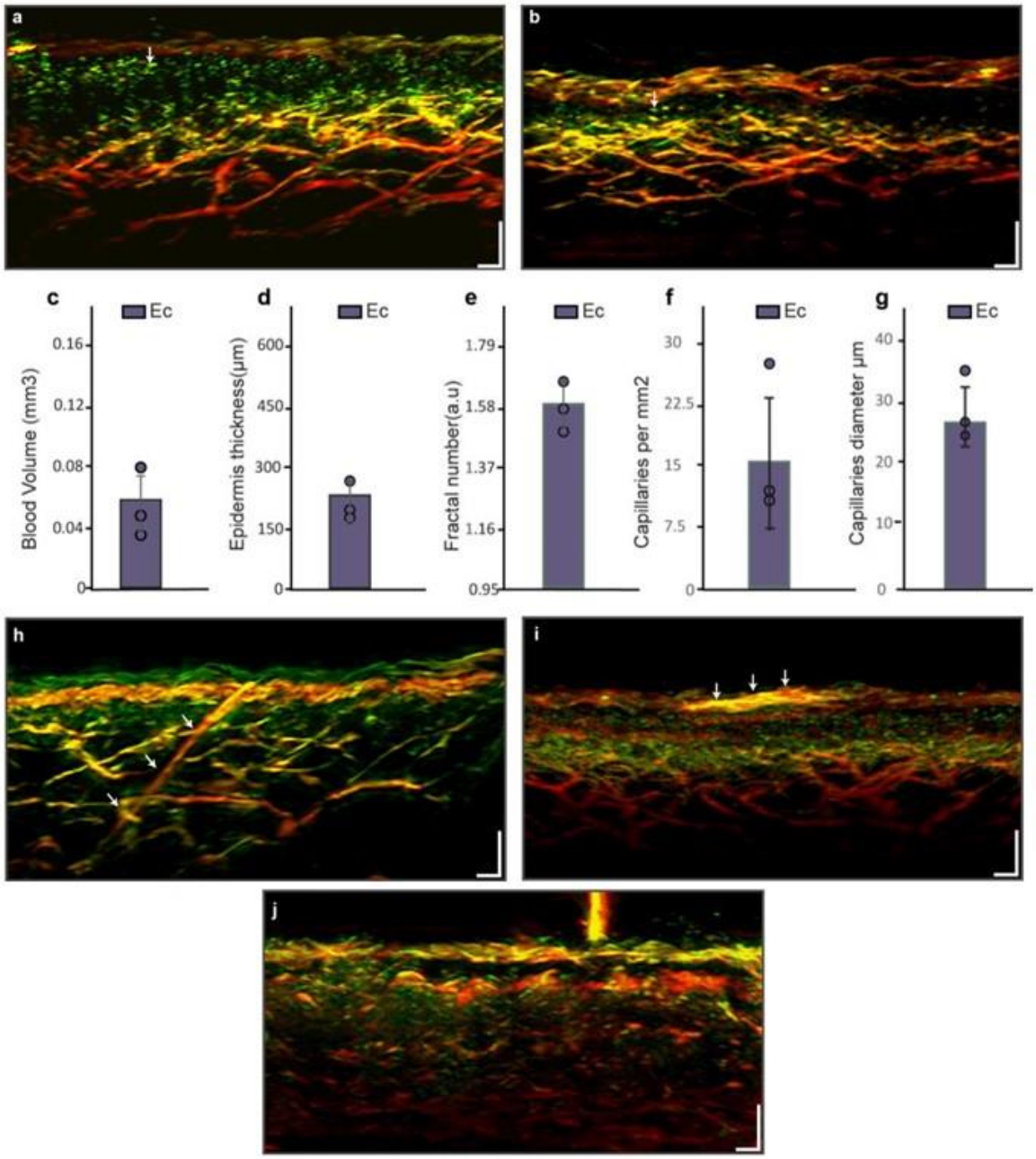

Figure 3 RSOM imaging of eczema and nevus a,b) Cross sectional images of skin regions affected by eczema. The tip of capillary loops that climb towards the surface appear in the images (white arrows) c-g) Measured values related to the vascular structure and epidermis thickness of three different eczema patients including the ones corresponding to figure a and b. h) Cross sectional image of healthy skin in which a hair shaft is displayed (white arrows) . i) Cross sectional image of a healthy skin region. A benign nevus is displayed (white arrows). j) Cross sectional image of a skin area affected by vasculitis. The vascular structure is completely distorted compared to the appearance of healthy skin. Scale bar: 200 µm.

5) System characterization

Both TUMs System 1 and iTheras system 2 share the illumination scheme and detection geometry. Therefore, the performance of the two systems is essentially similar.

We have characterized the lateral resolution (LR) and axial resolution (AR) of the lab system for the 10-180 MHz and the 10-120 MHz band implementation by imaging a 3.5 µm diameter carbon microsphere inserted in an agar based gelatin phantom at a depth of 300 µm. India ink and intralipid was added to the phantom in order to mimic the optical properties of tissue. We defined the LR taken as the FWHM of a profile of the microsphere in the lateral direction and the AR as the FWHM of a profile taken in the axial direction (Fig. 4a,b). For the 10-180 MHz implementation we obtained a LR of 18.4 µm and a AR 4.5 µm. For the 10-120 MHz implementation we obtained a LR of 29.6 µm and an AR 8.6 µm.

In order to characterize the possible degradation of the resolution as a function of depth, we imaged a USP 11-0 surgical suture (diameter ~10-19 µm) immersed in a phantom made from agar gelatin at different depths ranging from 350 µm to 2500 µm (~350 µm/upperdermis, ~800 µm/dermis and ~1500 µm/fat layer). Intralipid and ink were added to the gel in order to mimic the optical properties of tissue. At each depth, the profile of the suture was obtained in the lateral direction for the 10-180 MHz and the 10-120 MHz implementation. The FWHM of the profiles in the lateral direction at each depth were calculated (Fig. 4c). The degradation of the resolution at a certain depth can be characterized as difference in the FWHM obtained for the suture at such depth and the FWHM of the most superficial suture. While the resolution remained invariable through the whole depth of the dermis, certain degradation (~5 µm) could be observed at the depths corresponding to the fat layer.

We also characterized the sensitivity of the system when a vessel conforms a certain angle with the axial axis of the transducer (Fig. 4d). To do so, we built a phantom made out of agar and introduced a USP 11-0 surgical suture on it. The suture was rotated confirming different angles with regard to the axial axis of the transducer. For each angle, the sensitivity (sen) of the system was estimated (Fig. 4d-e). Such operation was done for the 10-180 MHz implementation and for 10-120 MHz implementation. From the suture reconstructed at different angles, the diameter was calculated as the FWHM of a profile in the direction of the axial axis of the suture (Fig. 4d) in the 10-120 MHz implementation. The maximum discrepancy was ~4µm.

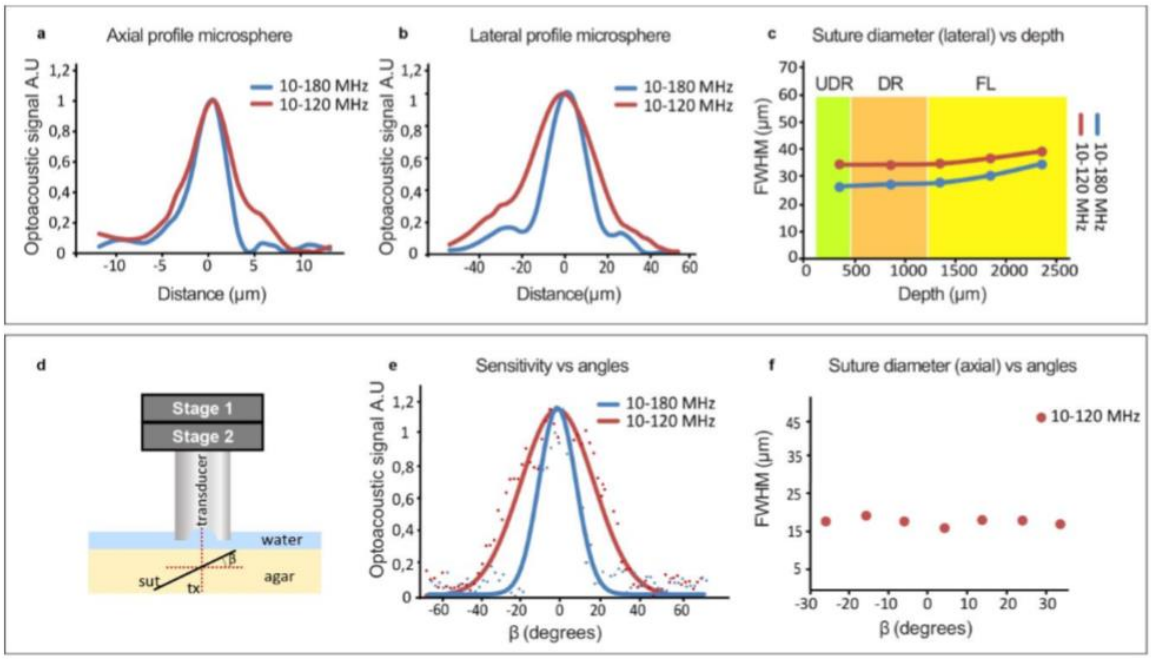

Figure 4: a)axial profile of a 3.5 µm diameter microsphere inserted in a tissue phantom at a depth of 300 µm obtained with the 10-180MHz and the 10-120 MHz implementation. b) lateral profile of a 3.5 µm diameter microsphere inserted in a tissue phantom at a depth of 300 µm obtained with the 10-180MHz and the 10-120 MHz implementation. c) FWHM obtained from a profile of a USP 11-0 suture taken in the lateral direction . The suture was placed at different depths in a tissue phantom. UDR corresponds to upper dermis, DR corresponds to dermis and FL corresponds to the fat layer. The FWHM maximum is constant through the whole skin depth d) scheme of the experimental set-up used to characterize the system performance when a vessel conforms a certain angle with the axial axis of the transducer. sut stands for suture, tx stands for the transducer axial axis and sx defines the suture axial axis. e) sensitivity of the system as function of the angle β as depicted in (d). f) FWHM of the suture in the axial direction obtained by the system in the 10-120 MHz implementation as function of the angle β as depicted in (d).

6) Future plans and conclusion

The described systems are backbone of the RSOM part of the INNODERM project. This system will be extensively used in clinics to determine the clinical abilities of RSOM. The systems will be improved in a continuous fashion in term of imaging performance and in term of usability, using the feedback from the clinical users.